

PAPER • OPEN ACCESS

## Kinematic origin for near-zero energy structures in mid-IR strong field ionization

To cite this article: Emilio Pisanty and Misha Ivanov 2016 *J. Phys. B: At. Mol. Opt. Phys.* **49** 105601

View the [article online](#) for updates and enhancements.

### Related content

- [Low-energy electron rescattering in laser-induced ionization](#)  
W Becker, S P Goreslavski, D B Milošević et al.
- [Keldysh theory of strong field ionization: history, applications, difficulties and perspectives](#)  
S V Popruzhenko
- [Atomic excitation and acceleration in strong laser fields](#)  
H Zimmermann and U Eichmann

### Recent citations

- [Analytic quantum-interference conditions in Coulomb corrected photoelectron holography](#)  
A S Maxwell *et al*
- [Coulomb-corrected quantum interference in above-threshold ionization: Working towards multitrajectory electron holography](#)  
A. S. Maxwell *et al*

# Kinematic origin for near-zero energy structures in mid-IR strong field ionization

Emilio Pisanty<sup>1,4</sup> and Misha Ivanov<sup>1,2,3</sup>

<sup>1</sup>Blackett Laboratory, Imperial College London, South Kensington Campus, SW7 2AZ London, United Kingdom

<sup>2</sup>Department of Physics, Humboldt University, Newtonstrasse 15, 12489 Berlin, Germany

<sup>3</sup>Max Born Institute, Max Born Strasse 2a, 12489 Berlin, Germany

E-mail: [e.pisanty11@imperial.ac.uk](mailto:e.pisanty11@imperial.ac.uk) and [m.ivanov@imperial.ac.uk](mailto:m.ivanov@imperial.ac.uk)

Received 27 November 2015, revised 15 February 2016

Accepted for publication 3 March 2016

Published 27 April 2016



CrossMark

## Abstract

We propose and discuss a kinematic mechanism underlying the recently discovered ‘near-zero energy structure’ in the photoionization of atoms in strong mid-infrared laser fields, based on trajectories which revisit the ion at low velocities exactly analogous to the series responsible for low-energy structures. The different scaling of the new series, as  $E \sim I_p^2/U_p$ , suggests that the near-zero energy structure can be lifted to higher energies, where it can be better resolved and studied, using harder targets with higher ionization potential.

Keywords: low-energy structures, near-zero energy structures, zero-energy structures, photo-ionization, strong-field physics, tunnel ionization

(Some figures may appear in colour only in the online journal)

The ionization of atoms in strong low frequency fields leads to rich structure in the low-energy part of the photo-electron spectrum. These structures, dubbed ‘low-energy structures’ (LES) [1, 2] and ‘very low energy structures’ (VLES) [3, 4], can contain about 50% of all electrons, and have recently been joined by a ‘near-zero energy structures’ (NZES) [5–8], opening interesting windows into the dynamics of electrons at the boundaries between classical and quantum dynamics.

The LES are peaks in the spectrum at constant longitudinal momentum, and they have been conclusively assigned to so-called soft recollisions [9, 10], in which the electron returns to the neighbourhood of its parent ion with a low or zero velocity. The VLES is a v-shaped pattern [4, 5, 7] caused by related mechanisms [11, 12], and has been tied with the LES as a single unified series of peaks [8–10] whose

energies scale linearly with the field’s ponderomotive energy  $U_p$  [13–15].

The NZES is a peak in the spectrum at much lower energies [5–8], experimentally consistent with zero kinetic energy for the photoelectron, and it is less well understood. One proposed mechanism is that low-energy electrons are trapped in Rydberg states at the end of the pulse [16, 17], and are subsequently ionized by the extraction fields of the detection apparatus [8, 18].

Here we propose a kinematic origin for the NZES that is exactly analogous to that responsible for the LES, and which places them at very small but positive energies [19]. We show that the soft recollisions that produce the LES series have a second branch at much lower energies and with a different scaling with the laser wavelength, intensity, and the ionization potential,  $I_p$ , of the target. For current experimental parameters the energies of this series are below the experimental resolution, so they appear consistent with zero energy. However, the particular scaling of this series, as  $I_p^2/U_p$ , suggests that experiments with targets that have a higher  $I_p$  can lift this series to higher energies, where they can be resolved and identified.

In contrast, the energies of the structures associated with ionization by the weak extraction field of the detection

<sup>4</sup> Author to whom any correspondence should be addressed.

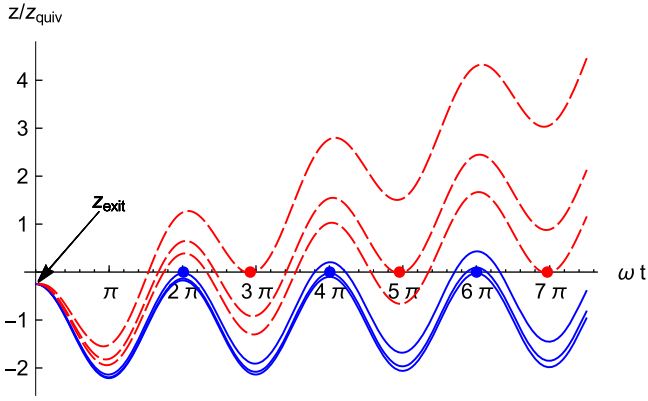


**Figure 1.** Trajectories with soft recollisions after tunnel ionization, for a Keldysh parameter of  $\gamma = 0.75$ .

apparatus should scale differently. In particular, the NZES yield would increase with stronger extraction fields, which should not affect direct-ionization mechanisms. This difference enables experimental testing of both pathways.

In the simplest model of tunnel ionization, an oscillating laser field  $\mathbf{F}(t) = F\hat{\mathbf{z}} \cos(\omega t)$  removes electrons by tilting the potential landscape around the atom to create a barrier that they can tunnel through. The electrons are then born near the peak of the field with zero velocity at the tunnel exit  $z_{\text{exit}} = F/I_p$ , and they propagate on classical trajectories driven by the laser field, oscillating with amplitude  $z_{\text{quiv}} = F/\omega^2$  around the uniform drift motion, until the pulse is over. (We use atomic units unless otherwise noted.) Within this model, the electron can approach the ion with near zero velocity in two dynamically different ways, depending on which side of the oscillation it does so, as shown in figure 1.

The LES are associated with trajectories with a soft recollision on a ‘backwards’ turning point [9, 10, 15], at times  $\omega t \approx (2k + 1)\pi$ , shown dashed in figure 1. These trajectories must advance by two quiver radii plus the tunnel exit over a fixed number of laser periods, which means that their drift momentum must scale as

$$p_z^{\text{sr}} = \frac{2z_{\text{quiv}} + z_{\text{exit}}}{\left(k + \frac{1}{2}\right)T} = \frac{F}{\omega} \frac{2 + \gamma^2/2}{(2k + 1)\pi} \propto \frac{F}{\omega}. \quad (1)$$

The energy is then a constant multiple of  $U_p = F^2/4\omega^2 \sim \gamma^{-2}$ , where  $\gamma = \omega\kappa/F$  is the Keldysh adiabaticity parameter. The tunnel exit contribution is the likely cause of the small observed deviations from this scaling [13–15], as confirmed by recent measurements [20]. This provides a look at the role of the tunnel exit in strong-field dynamics, analogous to similar corrections in the cutoff energies in high-order harmonic generation (HHG) [21] and high-order above-threshold ionization (ATI) [22, 23].

The ‘forwards’ turning points, on the other hand, are rather different. For a trajectory to recollide at zero velocity at times  $\omega t \approx 2\pi k$ , the drift momentum must only advance the electron by one tunnel exit over  $k$  periods:

$$p_z^{\text{sr}} = \frac{z_{\text{exit}}}{kT} = \frac{I_p/F}{2\pi k/\omega} \propto I_p \frac{\omega}{F}. \quad (2)$$

The energy scaling is now opposite to  $U_p$ , as  $E \sim I_p^2/U_p$ , and for current experimental parameters this energy is very small. For instance, for argon in a  $3.1 \mu\text{m}$  field of intensity  $10^{14} \text{ W cm}^{-2}$ , as in [6], the highest ‘forwards’ momentum is  $p_z^{\text{sr}} \approx 0.02 \text{ a.u.}$ , corresponding to an energy of 8 meV. This is consistent with the observed momentum spread of the NZES, and it is just below the current state of the art in detector momentum resolution.

This series appears to have remained undetected because the extent of the tunnelling barrier is generally much smaller than the quiver radius, so it is often neglected. However, in contrast to the ‘backwards’ series, and the HHG and ATI cutoff corrections, the tunnel-exit term for the ‘forwards’ series is a correction on zero, and it is now the leading term. As such, this series provides a more direct look at the tunnel exit, if it can be resolved.

Unfortunately, the scaling as  $E \sim \gamma^2 I_p$  of the ‘forwards’ series is rather unfavourable: on the one hand, it is desirable to maximize the energy of the series to bring it within reach of current detectors, but on the other it is necessary to make  $\gamma$  as small as possible to remain within the optical-tunnelling regime where the trajectory picture holds [8]. The role of this mechanism in the NZES, then, is best probed with experiments on high- $I_p$  targets such as He or He<sup>+</sup>. As a partial reprieve, the higher intensities required to ionize these targets allow one to reach the low- $\gamma$  regime at shorter wavelengths without incurring ionization saturation.

A slightly more formal treatment of the classical trajectories also permits both types of recollisions to be treated under a unified formalism. To do this one requires that both the position and the velocity of a classical trajectory [9] vanish, so

$$z_{\text{cl}}(t_r) = z_{\text{exit}} + \int_{t_0}^{t_r} (p_z + A(\tau)) d\tau = 0 \quad (3a)$$

$$v_z(t_r) = p_z + A(t_r) = 0, \quad (3b)$$

where  $A(t) = -\frac{F}{\omega} \sin(\omega t)$  is the vector potential of the system,  $z_{\text{exit}} = \text{Re} \left[ \int_{t_s}^{t_0} (p + A(\tau)) d\tau \right]$  is the tunnel length, and the tunnelling time  $t_s = t_0 + i\tau_T$  obeys  $\frac{1}{2}(p_z + A(t_s))^2 = -I_p$ . The solutions to these equations generally have a small reduced momentum  $\omega p_z/F$ , so one can linearize the equations to obtain a solvable system. The resulting soft-recollision momenta,

$$p_z^{\text{sr}} = \frac{F}{\omega} \frac{\sqrt{1 + \gamma^2} + (-1)^n}{(n + 1)\pi}, \quad (4)$$

include both the ‘forwards’ recollisions (when  $n = 2k$ ) and the ‘backwards’ series, for which  $n = 2k + 1$ ; this expression is valid for general  $\gamma$  as long as  $\omega p_z^{\text{sr}}/F \ll 1$ . These momenta, shown in figure 2, reduce to (1) and (2) in the limit of  $\gamma \ll 1$ .

Going beyond the simple man’s model, it is indeed possible to reproduce the NZES within semiclassical analytical theories; specifically, within the analytical  $R$ -matrix (ARM) theory of photoionization [24–29]. That formalism provides a first-principles basis for the inclusion of the Coulomb interaction of the photoelectron with the ion within a

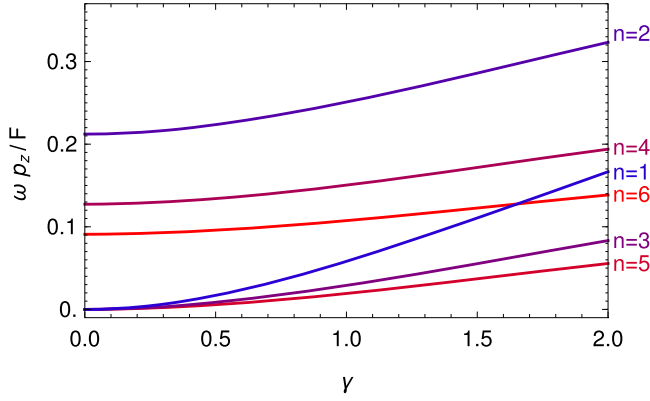


**Figure 2.** Scaling of the normalized momenta  $\omega p_z/F$  as a function of the Keldysh parameter,  $\gamma$ , for the first six soft-recollision trajectories, as per equation (4).

quantum-orbits framework [30, 31]. The ARM ionization amplitude is of the form

$$a(\mathbf{p}) = e^{i p_z t_s} e^{-\frac{i}{2} \int_{t_s}^T (\mathbf{p} + \mathbf{A}(\tau))^2 d\tau} \times e^{-i \int_{t_c}^T U(\int_{t_s}^{\tau} \mathbf{p} + \mathbf{A}(\tau') d\tau')} R(\mathbf{p}), \quad (5)$$

where  $R(\mathbf{p})$  is a form factor and  $U(\mathbf{r}) = -1/\sqrt{\mathbf{r}^2}$  is the Coulomb potential of the ion [19]. The effect of the ion is included at the level of the continuum wavefunction by using eikonal-Volkov solutions away from the molecule, and this modifies the standard results of the strong field approximation (SFA) by the inclusion of the phase  $e^{-i \int_{t_c}^T U(\mathbf{r}_{cl}(\tau)) d\tau}$ .

Within this framework, the imaginary part of the Coulomb action directly impacts the ionization amplitude, and its effect is magnified near a soft recollision as the electron spends a longer time in the neighbourhood of the ion. As shown in detail in [19], the soft recollision itself is associated with a sharp cliff in the ionization amplitude: the quantum Coulomb correction turns from enhancement at  $|p_z| < p_z^{\text{sr}}$  to suppression at  $|p_z| > p_z^{\text{sr}}$ , as a consequence of topological changes in the Coulomb potential's landscape and the resulting trajectory. At the precise momentum of the soft recollision, the ARM theory is likely to be at the edge of its domain of validity, but the change from ionization enhancement to suppression is likely to remain after the recollision is fully taken into account.

The resulting ARM ionization amplitude is characterized by a sharp cusp over the transverse momentum  $p_\perp$ , which is strictly localized in longitudinal momentum to momenta  $|p_z| < p_z^{\text{sr}}$  below the (corrected) soft recollision, as depicted in figure 3. This effect can be seen in the experimental spectra of [6], which show a Coulomb-focusing cusp [32] that is much more pronounced in the region of the NZES, sticking out of a Gaussian background.

As pointed out above, the key feature of the NZES is its scaling behavior. Figure 4 shows the quantum predictions based on the ARM approach, which closely follow the classical model.

Several mechanisms have been put forward to translate between a 'soft' approach to the ion and a peak in the

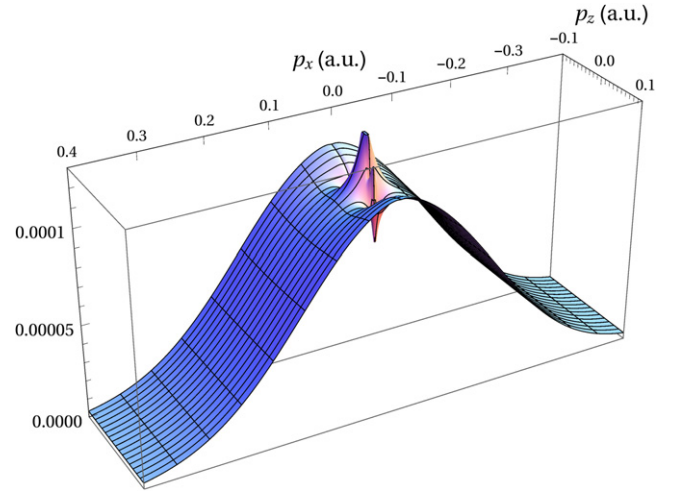


**Figure 3.** NZES structure in the photoelectron spectrum as calculated in [19] using analytical  $R$ -matrix techniques, for the experimental parameters of [6] (argon in a  $3.1 \mu\text{m}$  field at  $10^{14} \text{ W cm}^{-2}$ ). The increased time spent near the ion causes a cusp-shaped ionization enhancement that disappears abruptly as the enhancement briefly turns to suppression. (The dip, however, will likely be washed out in experiments.)

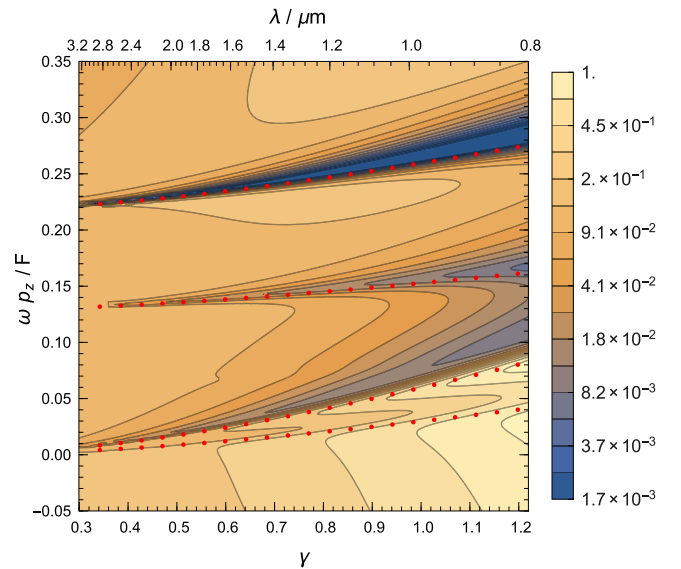


**Figure 4.** Dependence of the ARM ionization amplitude with  $\gamma$ , as calculated in [19]. The colour scale displays the ionization yield, in arbitrary units, coming from a single half-cycle for argon in a field of intensity  $9 \times 10^{13} \text{ W cm}^{-2}$  as the wavelength is varied. The transverse momentum is chosen so that the electron misses the core by a small but constant amount. The cusps of figure 3 appear as sharp drops in the yield, and these follow closely the scaling curves of figure 2, shown as dots for visibility.

photoelectron spectrum near that energy. Within the ARM theory, as well as analogous theories such as the Coulomb-corrected SFA (CCSFA) [33–35], the ionization enhancement comes about through a large imaginary action in a quantum-orbit formalism where time or the trajectory may be complex-valued. 'Improved' SFA models, which account for a single rescattering event [36–39], also reproduce the LES peaks, with large amplitudes fuelled by the divergent Coulomb

scattering cross-section. On another track, Monte Carlo classical simulations [14, 15, 40, 41] also reproduce the structure, where it appears as a result of dynamical focusing around the soft recollisions [9].

Nevertheless, it is important to point out that, whatever the mechanism is, the physics that ties the LES to the ‘backwards’ soft-recollision trajectories shown dashed in figure 1 should also be expected to do the same to the ‘forwards’ series, in the NZES energy range. In addition, a careful analysis of the different mechanisms at play in the LES shows that the Coulomb potential is crucial to bring out the feature, but that it is already embedded in the simple man’s model [38], which also puts the ‘forwards’ trajectories in the NZES energy range.

The effect of the Coulomb potential is also expected to affect the trajectory, by slowing the electron down as it leaves the atom, and this should be expected to shift the soft-recollision energies from the laser-driven positions as we have calculated them. As such, assessing the strength of this effect requires evaluation within frameworks such as CCSFA [33–35] which explicitly include the change in the trajectory, but in principle both effects should be present.

Similarly, if the pulse is short then its length, shape, and carrier-envelope phase will have a strong effect on the soft-recollision energies [10], separating the contributions from different periods and moving the LES and the NZES peaks as we have described them by potentially large shifts. The use of shape- and CEP-controlled short pulses to investigate these low-energy dynamical structures is a promising avenue which should resolve most of the open questions on the structures, but that amount of pulse-shape control in this intensity and wavelength range is still inaccessible to current sources. For the CEP-averaged sources in use, the effect of the pulse shape should average out to a result close to that for the monochromatic fields we consider.

On the other hand, the role of the extraction field  $F_{\text{ext}}$  in liberating Rydberg electrons should also be clarified, and it is possible that both the extraction-field and the kinematic mechanisms operate in tandem. Recent calculations [18] show that changes in the extraction field should indeed shift the peak, with support from experiments.

In addition to this effect, increases in the extraction field should also increase the yield of the structure: the Rydberg population density is expected to be constant at the small negative energies the small extraction field  $F_{\text{ext}} \sim 1 \text{ Vcm}^{-1} \approx 10^{-10}$  a.u. can probe [16, 17]. A larger field can probe a larger Rydberg energy range, and therefore expose a larger population. This effect, as yet unobserved, warrants further theoretical and experimental study, to clarify the contribution of the extraction field to the NZES.

The kinematic mechanism discussed here can similarly be probed by experiments, by testing the NZES’s scaling with respect to intensity, wavelength, and ionization potential. In practice, this requires a hard target with a high  $I_p$  and a strong field, to bring the ‘forwards’ series to higher energies where they can be resolved while keeping  $\gamma$  low.

As an example, experiments with helium at an intensity of  $3 \times 10^{14} \text{ W cm}^{-2}$  can keep  $\gamma = 0.83$  at a wavelength of

800 nm, and bring the ‘forwards’ soft-recollision momentum up to  $p_z^{\text{sr}} \approx 0.07$  a.u., for an energy of 68 meV. Ideally, experiments could use the helium ion, for which  $p_z^{\text{sr}} \approx 0.11$  a.u. (0.16 eV) at  $2.5 \times 10^{15} \text{ W cm}^{-2}$  and 400 nm, at the low  $\gamma$  of 0.43.

Such experiments are within the reach of current experimental capabilities, and they can explore the regimes where the NZES separates itself from zero. In addition, the ‘forwards’ soft-recollision trajectories explored here should also be present in streaking-based experiments [42], and they have a bearing on other low-energy ionization phenomena [43, 44] in this regime.

We thank L Torlina, O Smirnova, J Marangos, F Morales and W Becker for helpful discussions. EP gratefully acknowledges funding from CONACYT, and Imperial College London; MI and EP acknowledge support of EU-ITN CORINF and the EPSRC Programme Grant EP/I032517/1. The code and data used to produce the figures in this paper is available under a Creative Commons Attribution licence from [45].

## References

- [1] Blaga C I *et al* 2009 Strong-field photoionization revisited *Nature Phys.* **5** 335–8
- [2] Faisal F H M 2009 Strong-field physics: Ionization surprise *Nature Phys.* **5** 319–20
- [3] Quan W *et al* 2009 Classical aspects in above-threshold ionization with a midinfrared strong laser field *Phys. Rev. Lett.* **103** 093001
- [4] Wu C Y *et al* 2012 Characteristic spectrum of very low-energy photoelectron from above-threshold ionization in the tunneling regime *Phys. Rev. Lett.* **109** 043001
- [5] Dura J *et al* 2013 Ionization with low-frequency fields in the tunneling regime *Sci. Rep.* **3** 2675
- [6] Pullen M G *et al* 2014 Kinematically complete measurements of strong field ionization with mid-IR pulses *J. Phys. B: At., Mol. Opt. Phys.* **47** 204010
- [7] Wolter B *et al* 2014 Formation of very-low-energy states crossing the ionization threshold of argon atoms in strong mid-infrared fields *Phys. Rev. A* **90** 063424
- [8] Wolter B *et al* 2015 Strong-field physics with mid-IR fields *Phys. Rev. X* **5** 021034
- [9] Kästner A, Saalman U and Rost J M 2012 Electron-energy bunching in laser-driven soft recollisions *Phys. Rev. Lett.* **108** 033201
- [10] Kästner A, Saalman U and Rost J M 2012 Energy bunching in soft recollisions revealed with long-wavelength few-cycle pulses *J. Phys. B: At. Mol. Opt. Phys.* **45** 074011
- [11] Becker W and Milošević D B 2015 Above-threshold ionization for very low electron energy *J. Phys. B: At. Mol. Opt. Phys.* **48** 151001
- [12] Zhi-Yang L *et al* 2014 The Coulomb effect on a low-energy structure in above-threshold ionization spectra induced by mid-infrared laser pulses *Chin. Phys. B* **23** 023201
- [13] Guo L *et al* 2013 Scaling of the low-energy structure in above-threshold ionization in the tunneling regime: theory and experiment *Phys. Rev. Lett.* **110** 013001
- [14] Liu C and Hatsagortsyan K Z 2010 Origin of unexpected low energy structure in photoelectron spectra induced by midinfrared strong laser fields *Phys. Rev. Lett.* **105** 113003



- [15] Lemell C *et al* 2013 Classical-quantum correspondence in atomic ionization by midinfrared pulses: multiple peak and interference structures *Phys. Rev. A* **87** 013421
- [16] Nubbemeyer T *et al* 2008 Strong-field tunneling without ionization *Phys. Rev. Lett.* **101** 233001
- [17] Landsman A S *et al* 2015 Rydberg state creation by tunnel ionization *N. J. Phys.* **15** 013001
- [18] Diesen E *et al* Dynamical characteristics of rydberg electrons released by a weak electric field (arXiv:1507.06751)
- [19] Pisanty E and Ivanov M 2016 Slalom in complex time: emergence of low-energy structures in tunnel ionization via complex time contours *Phys. Rev. A* **93** 043408
- [20] Hickstein D D *et al* 2012 Direct visualization of laser-driven electron multiple scattering and tunneling distance in strong-field ionization *Phys. Rev. Lett.* **109** 073004
- [21] Lewenstein M *et al* 1994 Theory of high-harmonic generation by low-frequency laser fields *Phys. Rev. A* **49** 2117–32
- [22] Busuladžić M, Gazibegović-Busuladžić A and Milošević D B 2006 High-order above-threshold ionization in a laser field: influence of the ionization potential on the high-energy cutoff *Laser Phys.* **16** 289–93
- [23] Frolov M V, Manakov N L and Starace A F 2009 Analytic formulas for above-threshold ionization or detachment plateau spectra *Phys. Rev. A* **79** 033406
- [24] Torlina L and Smirnova O 2012 Time-dependent analytical R-matrix approach for strong-field dynamics I. One-electron systems *Phys. Rev. A* **86** 043408
- [25] Kaushal J and Smirnova O 2013 Nonadiabatic Coulomb effects in strong-field ionization in circularly polarized laser fields *Phys. Rev. A* **88** 013421
- [26] Torlina L, Morales F, Muller H G and Smirnova O 2014 *Ab initio* verification of the analytical R-matrix theory for strong field ionization *J. Phys. B: At. Mol. Opt. Phys.* **47** 204021
- [27] Torlina L, Kaushal J and Smirnova O 2013 Time-resolving electron-core dynamics during strong-field ionization in circularly polarized fields *Phys. Rev. A* **88** 053403
- [28] Torlina L *et al* 2015 Interpreting attoclock measurements of tunnelling times *Nature Phys.* **11** 503–8
- [29] Pisanty E 2012 Under-the-barrier electron-ion interaction during tunnel ionization *MRes Report* (Imperial College London) (arXiv:1307.7329)
- [30] Salières P *et al* 2001 Feynman's path-integral approach for intense-laser-atom interactions *Science* **292** 902–5
- [31] Popov V 2005 Imaginary-time method in quantum mechanics and field theory *Phys. Atom. Nucl.* **68** 686–708
- [32] Rudenko A *et al* 2005 Coulomb singularity in the transverse momentum distribution for strong-field single ionization *J. Phys. B: At., Mol. Opt. Phys.* **38** L191
- [33] Popruzhenko S V, Paulus G G and Bauer D 2008 Coulomb-corrected quantum trajectories in strong-field ionization *Phys. Rev. A* **77** 053409
- [34] Popruzhenko S and Bauer D 2008 Strong field approximation for systems with Coulomb interaction *J. Mod. Opt.* **55** 2573–89
- [35] Yan T-M, Popruzhenko S V, Vrakking M J J and Bauer D 2010 Low-energy structures in strong field ionization revealed by quantum orbits *Phys. Rev. Lett.* **105** 253002
- [36] Milošević D B 2013 Reexamination of the improved strong-field approximation: Low-energy structures in the above-threshold ionization spectra for short-range potentials *Phys. Rev. A* **88** 023417
- [37] Milošević D B 2014 Forward- and backward-scattering quantum orbits in above-threshold ionization *Phys. Rev. A* **90** 063414
- [38] Becker W, Goreslavski S, Milošević D B and Paulus G 2014 Low-energy electron rescattering in laser-induced ionization *J. Phys. B: At. Mol. Opt. Phys.* **47** 204022
- [39] Möller M *et al* 2014 Off-axis low-energy structures in above-threshold ionization *Phys. Rev. A* **90** 023412
- [40] Liu C and Hatsagortsyan K Z 2011 Wavelength and intensity dependence of multiple forward scattering of electrons at above-threshold ionization in mid-infrared strong laser fields *J. Phys. B: At. Mol. Opt. Phys.* **44** 095402
- [41] Liu C and Hatsagortsyan K Z 2012 Coulomb focusing in above-threshold ionization in elliptically polarized midinfrared strong laser fields *Phys. Rev. A* **85** 023413
- [42] Xu M-H *et al* 2011 Attosecond streaking in the low-energy region as a probe of rescattering *Phys. Rev. Lett.* **107** 183001
- [43] Arbó D G *et al* 2006 Interference oscillations in the angular distribution of laser-ionized electrons near ionization threshold *Phys. Rev. Lett.* **96** 143003
- [44] Rudenko A *et al* 2004 Resonant structures in the low-energy electron continuum for single ionization of atoms in the tunnelling regime *J. Phys. B: At. Mol. Opt. Phys.* **37** L407
- [45] Pisanty E 2016 Figure-maker code for Slalom in complex time: emergence of low-energy structures in tunnel ionization via complex time contours, and kinematic origin for near-zero energy structures in mid-IR strong field ionization (doi:10.5281/zenodo.46912)